QUARTERLY JOURNAL OF THE ROYAL METEOROLOGICAL SOCIETY
Q. J. R. Meteorol. Soc. **135**: 353–370 (2009)
Published online in Wiley InterScience
(www.interscience.wiley.com) DOI: 10.1002/qj.384

Large-scale controls on Ganges and Brahmaputra river discharge on intraseasonal and seasonal time-scales

Jun Jian, Peter J. Webster* and Carlos D. Hoyos
School of Earth and Atmospheric Sciences, Georgia Institute of Technology, Atlanta, Georgia, USA

ABSTRACT: Reliable water supply from the Ganges and Brahmaputra is of critical importance to the sustainability of the agricultural societies of India and Bangladesh. But, the flow in both basins is highly variable on time-scales ranging from days to years, creating challenges for the optimization of agricultural practices, water resource management and disaster mitigation. The following questions are addressed. Is intraseasonal monsoon variability related to the subseasonal variability of river flow? Do variations in the large-scale tropical sea-surface temperature (SST) located both regionally and remotely promote seasonal and interannual variations of river discharge? And, if these relationships do exist, are they determinable with sufficient lead-times to allow useful predictions for user communities in South Asia? We examine these questions using 50 years of daily river discharge data for both rivers calculated at the points where they enter Bangladesh, and with SST data in the Indo-Pacific region. We also examine the question of determining the impact of man-made dams, diversions and barrages on the data record, especially that of the Ganges. A comparison of discharge prior to 1974 (the time of the construction of the largest barrage) shows no statistical difference that cannot be explained by basin-wide rainfall distributions. Changes that do occur are restricted to the dry-season months.

Subseasonal river discharge is found to be strongly tied to the monsoon intraseasonal cycle resulting in a near-in-phase timing of Ganges and Brahmaputra discharge. A basin isochrone analysis is used to couple stream-flow variability and intraseasonal precipitation during the different phases of the intraseasonal cycle. On longer time-scales, statistically significant correlations are found between mean monthly equatorial Pacific SST and the boreal summer Ganges discharge with lead times of 2–3 months. These relationships are tied to El Niño–Southern Oscillation (ENSO) oscillations in addition to SST variability in the southwest and northwest Pacific that also seems to be related to ENSO. The Brahmaputra discharge, on the other hand, shows somewhat weaker relationships with tropical SST. Strong lagged correlation relationships are found with SST in the Bay of Bengal but these are the result of very warm SSTs and exceptional Brahmaputra discharge during the summer of 1998. When this year is removed from the time series, relationships with SST anomalies weaken everywhere except in the northwest Pacific for the June discharge and in areas of the central Pacific straddling the Equator for the July discharge. In addition, the northwest Pacific relationship changes polarity for June and July discharges. Although the relationships are weaker than those found for the Ganges, they are persistent from month to month and suggest that two different and sequential factors influence Brahmaputra river flow. Copyright © 2009 Royal Meteorological Society

KEY WORDS predictability; rainfall–discharge–SST relationship

Received 19 December 2007; Revised 1 January 2009; Accepted 5 January 2009

1. Introduction

Accurate and timely forecasts of river flow have the potential of providing critical information for water resource management, agriculture optimization and disaster mitigation. Nowhere is the need for reliable and timely forecasts more urgent than in the Bangladesh delta fed by two of the largest river systems in the world: the Brahmaputra and Ganges (Figure 1(a)). The catchment area of the Ganges system extends across the great plains of northern India beginning in Nepal and along the southern slopes of the Himalaya. The Brahmaputra basin extends northward through Assam and Bhutan and then westward into the Himalayas and the Tibetan Plateau. River flow through Bangladesh, located at the confluence of these two great rivers, is fed by a combined catchment area that ranks tenth in size on the planet. Only the Amazon and the Congo surpass the combined climatological flow of the two rivers.

Each year, short-lived flooding occurs throughout the summer and early autumn but with sufficient irregularity to have adverse agricultural and societal consequences and disruptions to social and agricultural activities. Major flooding events occur in Bangladesh every five years or so. For example, in the summer of 1998 over 60% of Bangladesh was inundated for nearly three months (Chowdhury, 2003; Mirza *et al.*, 2003). The summers of 1987 and 1988 also brought devastating floods of similar extent and duration. In 2004 and twice during 2007, the Brahmaputra flooded large areas of Bangladesh for periods between 1 and 2 weeks. Given the consequences of major flooding, the rationale for developing accurate forecast schemes is obvious. Furthermore, the forecasting of the location and timing of the smaller floods 10–30 days in advance can allow advantageous changes in planting,

*Correspondence to: Peter J. Webster, 311 Ferst Drive, Atlanta, GA 30332, USA E-mail: pjw@eas.gatech.edu

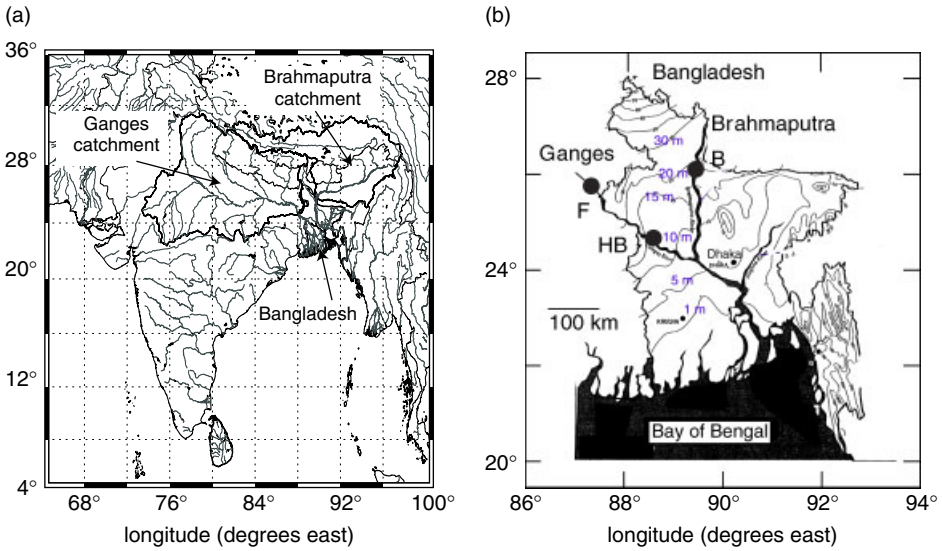

Figure 1. The Brahmaputra and Ganges systems. (a) The catchment areas of the Brahmaputra and Ganges Rivers (solid outlines), and (b) detailed map of Bangladesh and the entrance points of the Brahmaputra and Ganges Rivers into the country where river flow measurements are made. The locations of the two staging stations within Bangladesh, Bahadurabad and Hardinge Bridge, are denoted by 'B' and 'HB' next to solid circles, respectively. 'F' denotes the Indian Farakka Barrage. Isopleths show elevation above mean sea-level (m). This figure is available in colour online at www.interscience.wiley.com/journal/qj

harvesting, fertilizing and pest control (Subbiah, 2004; Webster *et al.*, 2006).

The Bangladesh prediction problem is especially acute because no upstream river flow data, either current or historical, is available from India where the catchments of the Ganges and Brahmaputra largely reside. Furthermore, only a limited amount of precipitation data is available to Bangladesh with a lead-time necessary for utilization. The only information of river discharge available to Bangladesh is that which is calculated directly by the Bangladeshis themselves at the locations where the two rivers enter Bangladesh from India (Figure 1(b)). As a result, authorities in Bangladesh have been restricted to issuing forecasts extending out to two days, matching the transit time of river flow through Bangladesh. Near the entry points of the rivers into Bangladesh, there is little forecast lead-time at all. Despite efforts to produce longer-term forecasts of river discharge, the lack of upstream data has been crippling. From a Bangladeshi perspective, the upstream Ganges and Brahmaputra catchments must be considered as the two largest un-gauged river basins on the planet. Without upstream data, short-term forecasting of river discharge (1–10 days) requires forecasting precipitation and other weather variables over the entire extent of the basins to initialize hydrological models (Hopson and Webster, 2009). Thus, it is important to investigate whether longer-term empirical forecasts are possible through associations with climatic oscillations possessing predictable elements on intraseasonal and seasonal time-scales.

Most studies seeking predictable elements of river discharge have concentrated on the association of large-scale and easily identifiable climate indices such as the Southern Oscillation Index (SOI). Amarasekera *et al.* (1997), for example, related interannual Pacific Ocean SST variability with the discharge of two tropical rivers, the Congo and the Amazon, and two subtropical rivers, the Parana and the Nile. The Amazon and Congo appeared weakly and negatively correlated with the SOI with only 10% of the variance explained. The Nile and Parana, on the other hand, had twice the variance explained by the SOI, correlating negatively with the Nile and positively for the Parana. Berri *et al.* (2002) studied the Parana–La Plata complex and noted that during the El Niños of 1983, 1992 and 1998 excessive flooding occurred requiring the evacuation of hundreds of thousands of people. Wang and Eltahir (1999), Tawfik (2003) and Eldaw *et al.* (2003) have corroborated the Nile discharge–SOI association. Labat *et al.* (2004, 2005) using wavelet techniques showed that the Amazon, Parana, Orinoco and Congo river flows were influenced by the SOI on a 3–6-year time-scale in keeping with the earlier study of Amarasekera *et al.* (1997), while longer term variability was influenced by a combination of the Pacific Decadal Oscillation and the North Atlantic Oscillation.

Whitaker *et al.* (2001), concentrating on the Ganges, found a relatively strong relationship at the 95% significance level between annual river flow and indices of the extremes of El Niño–Southern Oscillation (ENSO) and also whether the trend of the SOI was increasing or decreasing, suggesting that there existed a basis for prediction. These encouraging results are in agreement with the relatively strong relationship between total Indian rainfall and ENSO (e.g. Shukla and Paolino, 1983; Yasunari, 1990; Shukla, 1995) although its stationarity is questioned by the apparent waning of Indian monsoon precipitation–ENSO relationships during the last few decades (Torrence and Webster, 1998, 1999; Kumar *et al.*, 1999; Stephenson *et al.*, 1999; Clark *et al.*, 2000, 2003). However, other studies using different proxies of the Indian monsoon suggest the relationship with ENSO is still significant (Gershunov *et al.*, 2001; Goswami and

DOI: 10.1002/qj

Xavier, 2005; van Oldenborgh and Burgers, 2005). The question of whether a trend exists in the ENSO–monsoon relationship is compounded by Gershunov *et al.* (2001) who contend that it is impossible to separate a change in the ENSO–monsoon relationship because of the statistical noise in the system. Perhaps the problem of discerning a signal arises because the monsoon also may impact ENSO as well (e.g. Normand, 1953; Webster and Yang, 1992).

Chowdhury (2003) and Chowdhury and Ward (2004) extended the Ganges analysis to the Brahmaputra and the Meghna (Figure 1). Shaman *et al.* (2005), concentrating on the Brahmaputra, included an assessment of the importance of springtime Himalayan and Tibetan Plateau snow pack. Chowdhury and Ward (2004) found correlations between rainfall in the upper reaches of the Ganges and Brahmaputra catchment areas and the subsequent river discharge into Bangladesh. However, there was no categorization in terms of seasonal monsoon modes defined by 'active' (rainy) and 'break' (dry) periods (e.g. Webster *et al.*, 1998; Lawrence and Webster, 2001, 2002) and a possible subseasonal variability of river discharge. Given that the active and break sequences follow a relatively robust pattern (Lawrence and Webster, 2002) and possess considerable predictability (Webster and Hoyos, 2004), the determination of a relationship between the phase of the monsoon intraseasonal variability and river discharge would appear to be potentially fruitful.

Chowdhury and Ward (2004) also correlated river discharge in different months with simultaneous distributions of SST in the Indo-Pacific region, finding (1) the Ganges River flow correlates negatively with eastern–central Pacific SSTs and positively with the western Pacific SSTs, probably under the ENSO influence and (2) the Brahmaputra discharge does not appear to have any direct relationship with the central–eastern Pacific SSTs, a result substantiated by Shaman *et al.* (2005), for both the river discharge and Bangladesh rainfall. The latter result appears to be consistent with Shukla (1995) who found decreasing correlations between the SOI and rainfall from the western part of the Ganges Valley (maximum) to Bangladesh (minimum). Positive correlations were found by Chowdhury and Ward (2004) between Brahmaputra discharge and north Indian Ocean and west Pacific SSTs. Later, we will question the robustness of the role of the north Indian Ocean SST found by Chowdhury and Ward (2004). Finally, although extremely limited by a short data record (9 years), Shaman *et al.* (2005) suggested that the Brahmaputra discharge was related to Himalayan snow depth during the previous spring.

The purpose of this note is to determine whether or not there are useful signals in the evolving climate system on time-scales ranging from intraseasonal to interannual that would aid in the long-term prediction of river flow levels in the Brahmaputra–Ganges River delta. In the next section, a description of the data used in the study is presented. A discussion of the temporal scales of variability of the Ganges and Brahmaputra river discharge is given in section 3. Here, the impact of man-made artefacts on river flow (dams, barrages and diversions) is also considered. In sections 4 and 5, the intraseasonal, seasonal and annual variation of Ganges and Brahmaputra river discharge is examined, together with their relationship to broad climate metrics. Section 6 summarizes results, suggests a number of extensions and discusses the utility of the results.

2. Data

The discharge data used in this study is derived from the water levels measured at staging stations at Bahadurabad on the Brahmaputra River, and at Hardinge Bridge on the Ganges. Both stations lie close to the Bangladesh–Indian border (marked with arrows in Figure 1(b)). Daily Ganges and Brahmaputra discharge data used in the study extend from 1950 to 2003 and 1956 to 2003, respectively. Isolated missing data points are replaced by linear interpolation. Longer missing periods (several winters and summer 1971) were not considered in subsequent correlation analysis and time series.

SST data are retrieved from the National Oceanic and Atmospheric Administration (NOAA) Extended Reconstructed SST dataset (Smith and Reynolds, 2003). The data are compiled using the most recently available Comprehensive Ocean–Atmosphere Data Set (COADS) SST data and improved statistical methods that allow for stable reconstruction of sparse data. This monthly mean analysis commences in January 1854 and extends to December 2003 with a resolution of $2^\circ \times 2^\circ$ latitude–longitude. Here, only the period from 1950 to 2003 is considered to match the discharge data. Also, because of the paucity of SST data in some regions of the Tropics and Southern Hemisphere, we apply a criterion that within an analysis square there must be at least the mean number of data points less one-half standard deviation of the 1996–2005 values for the data to be useful for our purposes. SST data in the Pacific and Indian Oceans for the period 1950 to the present fit this criterion. Estimates of precipitation are obtained from a satellite-based global precipitation analysis provided by the Global Precipitation Climatology Project (GPCP: Arkin and Meisner, 1987; Adler *et al.*, 2003). Pentad rainfall estimates are available from 1979 to 2005 and daily data from 1996 to 2004. Exceptionally, the averaged Ganges basin rainfall is calculated from a high-resolution gridded one-degree daily rainfall data compiled by Rajeevan *et al.* (2005, 2006).

Finally, we construct basin isochrone maps for interpretation of river flow rates and the determination of hydrological time-scales for the two basins. Isochrones are estimated by first using a flow-routing algorithm (Ramirez and Vélez, 2002) and a regional digital elevation model (DEM) of the region to find the path and the distance of every grid cell to the outflow of the basin. The regional DEM for the Ganges and Brahmaputra basins was extracted from a global DEM (GTOPO30) with horizontal resolution of 30 arc-seconds (approximately 1 km). The simplest way to estimate isochrones is by assuming constant average flow velocity within the entire basin network, including hill slopes and channels.

DOI: 10.1002/qj

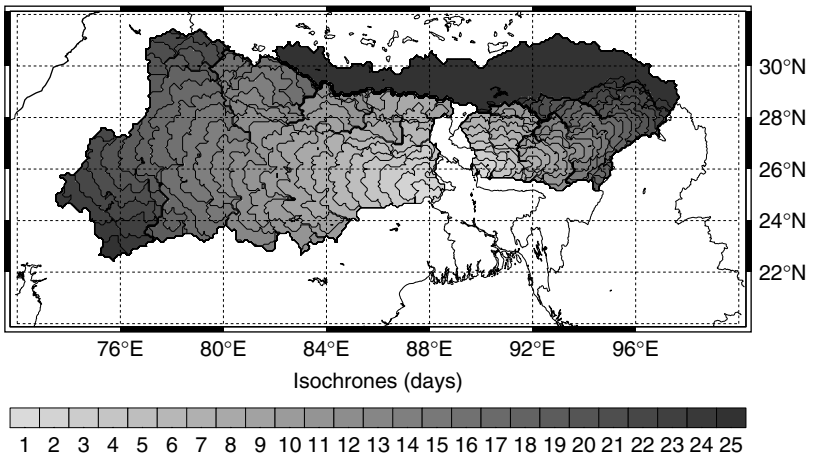

Figure 2. Isochrones (days) for the Brahmaputra and Ganges basins. The contours provide an estimate of the time it takes for water in a particular location in the basin to pass to Bahadurabad and Hardinge Bridge, the staging stations shown in Figure 1(b). Numbering refers to isochrone day.

For detailed applications, further hydraulic and terrain considerations are necessary to estimate the network flow velocity, which is probably different at every grid cell. However, for the purpose of this study, and given the spatial (1 degree $\sim$ 120 km) and temporal (daily) resolution of the rainfall, 1 m s^{-1} is a reasonable assumption for both basins given their average slope and land cover (e.g. Chow *et al.*, 1988). Figure 2 shows isochrones in units of days for both the Ganges and Brahmaputra basins. Isochrones should be interpreted as indicative of the average time it takes a parcel of liquid water located in some location within the basin to reach the outlet of the basin.

3. Temporal variability in Ganges and Brahmaputra discharge

Figure 3(a) shows 11 years of the 50 plus years of Brahmaputra and Ganges discharge data described above. The time series shows high magnitude interannual variability and, within each year, subseasonal variance. The inset panel shows the annual cycles of both river flows measured at the India–Bangladesh border from 1956 onwards.

The annual cycles of discharge (inset: Figure 3(a)) indicate significant phase differences. The Brahmaputra flow increases rapidly in late spring, ahead of the Ganges by about two months, probably for two reasons. First there is springtime snowmelt from the Himalayas and Tibetan Plateau that runs fairly unattenuated to the Bay of Bengal. Early Ganges discharge also depends on snowmelt in the Nepalese Himalaya occurring at roughly the same time as at the head of the Brahmaputra basin. But, residing between Nepal and Hardinge Bridge within the Ganges Valley are 10% of the global population that uses much of the early Ganges discharge for irrigation and the refilling of dams and other water diversions. Thus, part of the differences in the annual cycles of the two rivers is probably the signature of extreme human activity, plus the different basin time-scales (Figure 2). Second, rains generally occur in Assam (to the northeast of Bangladesh) some weeks earlier than over the Ganges catchment (Webster *et al.*, 1998; Lawrence and Webster, 2002). Thus, there are climatological reasons why the differences in the annual cycles of the two rivers cannot be explained solely in terms of hydrological time-scales calculated from the isochrone analysis. If this were true, the isochrone analysis of the Brahmaputra would have to be in error by a factor of 8.

A time series of annual mean discharge for each of the rivers is shown in Figure 3(b). The long-term mean annual discharge for the Brahmaputra is 2.01×10^4 m^3 s^{-1} compared to 1.14×10^4 m^3 s^{-1} for the Ganges. The cumulative discharge (Figure 3(c)) indicates considerable interannual variability in the discharge of both the Ganges and the Brahmaputra rivers. Between 1988 and the present, the Brahmaputra discharge has been well above average. The Ganges, on the other hand, has shown a steady decrease in discharge since the 1960s perhaps due to the combination of decrease in the strength of the overall Indian monsoon since the early 1970s (e.g. Webster *et al.*, 1998) and other non-natural factors.

One possible reason for the multi-decadal flow characteristics could be the influences of man through the construction of river diversions such as dams and barrages and the increasing use of water for irrigation with a rising population. The Brahmaputra remains largely uncontrolled whereas in the Ganges basin there have been a number of major hydrological projects. The largest is the Farakka Barrage, constructed in 1974–1975 and located just 10 km from the border with Bangladesh (see Figure 1(b)). The dam was built to divert the Ganges River water into the Hooghly River during the dry season (January to June) in order to flush out the accumulated silt that in the 1950s and 1960s was a problem at the major port of Kolkata (Calcutta) which lies on the Hooghly River. Noting this issue, we compare the climatological precipitation derived from the $1^\circ \times 1^\circ$ dataset of Indian daily rainfall and river discharge at Hardinge Bridge (see Figure 1(b)) over the periods before and after 1975. These comparisons are shown in Figure 4(a) and (b), respectively. The Ganges basin (76 °E–88 °E, 24°N–29°N) precipitation annual cycles for the two periods differ little

DOI: 10.1002/qj

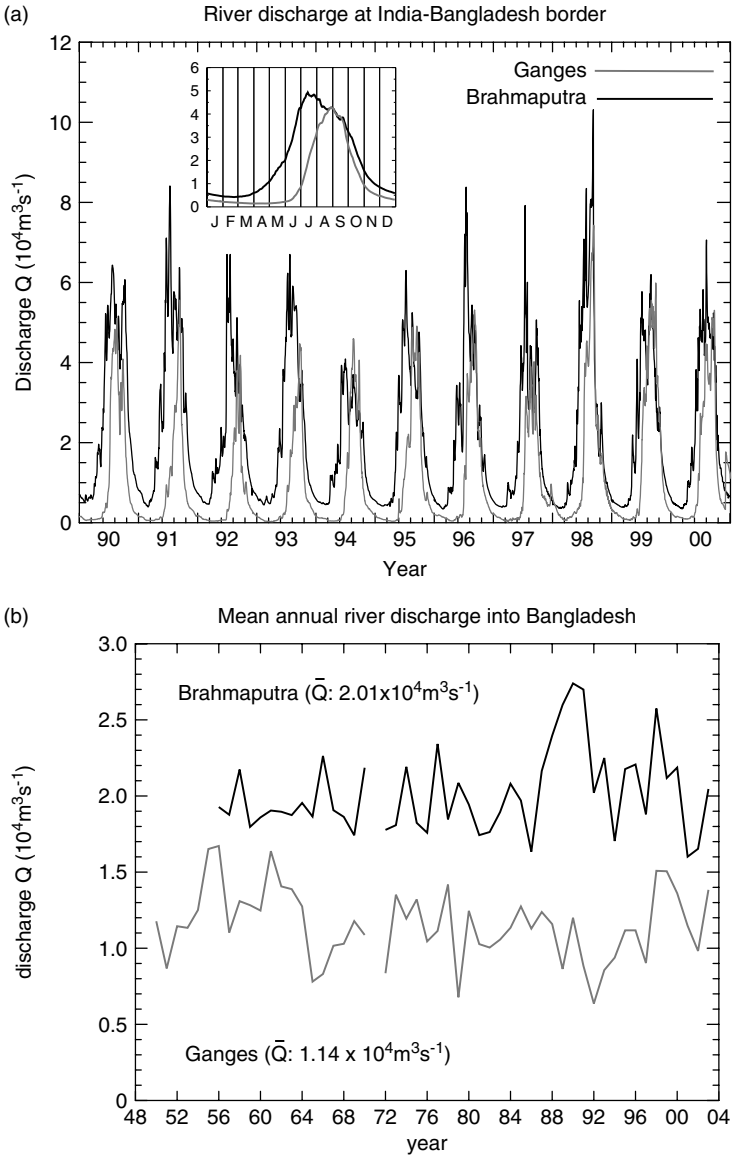

Figure 3. (a) The discharges of the Brahmaputra (black) and the Ganges (grey) Rivers retrieved from Bahadurabad and Hardinge Bridge stations respectively, for 11-year period (1990–2000). Inset shows the mean annual cycle of discharge of both rivers calculated over the entire length of the dataset. (b) Mean annual discharge of the Brahmaputra (black) and Ganges (grey) for the periods 1950 to 2003 and 1956 to 2003, respectively. (c). Cumulative river discharge for the Brahmaputra (black) and Ganges (grey).

for all months except August that shows a 6% reduction after 1975. Similarly, the two mean discharge annual cycles (Figure 4(b)) differ little as well, showing, though, that the reduced August rainfall corresponds to a slightly lower August discharge. The only significant differences in terms of percentage of mean monthly flow occur during the monsoon dry season (November through to May) when water is diverted to the Hooghly. As our major interest is in the wet season discharge, we conclude that human influences are indiscernible during the wet season from variations in the precipitation record throughout the period of the data record both prior to and after the construction of the Farakka Barrage.

River stream-flow is highly correlated with precipitation occurring at locations higher up in the catchment basin as shown by Chowdhury and Ward (2004). In the Southeast Asian monsoon region, rainfall shows strong intraseasonal variability (30–80 days) during the wet season that results in active and break phases of the monsoon (e.g. Sikka and Gadgil, 1980; Webster *et al.*, 1998; Lawrence and Webster, 2000, 2002). Discharge of rivers Ganges and Brahmaputra also shows variability in the intraseasonal band that explains about 10% of the daily discharge variance, a considerable amount considering the large amplitude of the annual cycle. Figure 5 shows details of the year 1998 for both rivers. Early season discharges were close to climatology in each river. However, by mid-June, the Brahmaputra continued to rise so that by the end of July the discharge was almost twice that of climatology. Peak flows occurred in mid-September with discharges nearly three times the September climatological values. The Ganges also peaked at the same time with double climatological values.

DOI: 10.1002/qj

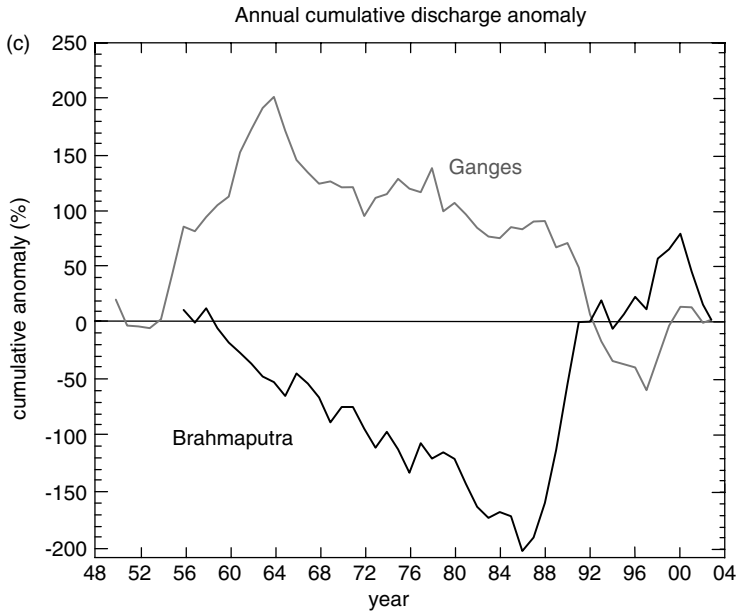

Figure 3. (*Continued*)

In addition to year-to-year variability, Ganges and Brahmaputra discharge is strongly modulated by the marked intraseasonal variability present within the wet season of the Southeast Asian monsoon (Lawrence and Webster, 2002; Webster and Hoyos, 2004). The observed rainfall and river discharge intraseasonal variability over Southeast Asia appears as a result of the large-scale intraseasonal modulation of convection over the Indian Ocean and its associated northward propagation of convective anomalies (Hoyos and Webster, 2007) that correspond to the summer manifestation of the Madden–Julian Oscillation (e.g. Madden and Julian, 1994). Figure 6(a) shows a plot of Ganges discharge at Hardinge Bridge and precipitation averaged over the Ganges basin for 1997. In addition to the high frequency variability of daily rainfall (thin dashed line), there is a low varying envelope brought out by a 10-day moving average of rainfall (thick dashed line) associated with periods of above and below normal rainfall associated with the active and break periods. While most of the high-frequency rainfall variability is not evident in the discharge record of the Ganges (black continuous line), because of the low-pass filter effect of the basin, the correspondence between the intraseasonal rainfall and discharge peaks is very high (0.6 correlation) with rainfall variability leading discharge variability by $\sim$13 days. To illustrate the correspondence, the low-pass rainfall distribution is displaced by 13 days (Figure 6(b)). The correspondence is a common feature for all years since 1997 when the daily GPCP rainfall product became available with correlations for each year varying from 0.5 to 0.65 and lead-times between 12 and 17 days. In the next section, we use band-pass filtering, composite and correlation analysis methods to study the intraseasonal precipitation–discharge relationship in more detail

4. Intraseasonal variability of Ganges and Brahmaputra discharge

A composite analysis of daily intraseasonal discharge variability reveals an almost in-phase relationship between the two rivers (not shown). The composite variability was constructed based on 27 active events of Ganges discharge from 1996 to 2004 obtained from filtered daily time series in the 15–60-day spectral band. For the purposes of the analysis, an 'active' event is defined as a period of maximum discharge in the 15–60-day band with a magnitude greater than one standard deviation of the mean variance within the band.

In order to establish the link between Ganges and Brahmaputra discharge and intraseasonal rainfall variability, composites of daily GPCP rainfall were constructed. Figure 7(a) shows the evolution of the composite from day -20 to day 5. The sequence illustrates maximum rainfall anomalies over both basins about 15 to 20 days prior to the maximum discharge in the Ganges. An interesting spatial progression appears over the Ganges basin. Positive rainfall anomalies over the Ganges basin occur before the peak discharge in the farthest reaches of the basin outlet around day -20, and move closer towards the outlet as time progresses. A similar progression is observed for the Brahmaputra catchment for composites constructed similarly using active events based on Brahmaputra discharge (Figure 7(b))

The spatial progression of the rainfall anomalies provides an explanation of the low-pass filter effect introduced by the basin and the related change in the intraseasonal spectral peak. The composites show that the river discharge in both basins lags the peak intraseasonal oscillation (ISO) rainfall by about 20 days over the Bay of Bengal, which, in itself, is useful for discharge prediction. The memory introduced by the basin relative to the arrival of the large-scale intraseasonal active event is an

DOI: 10.1002/qj

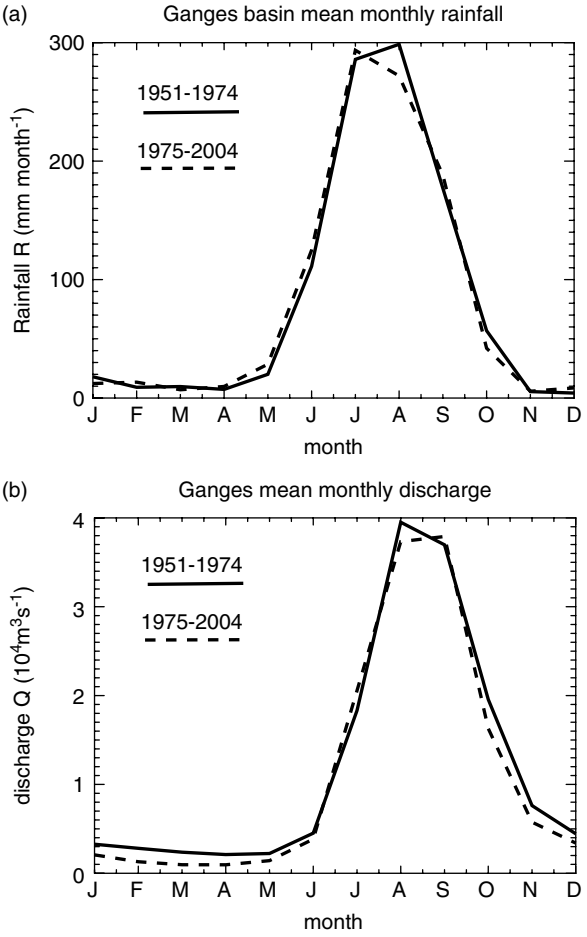

Figure 4. (a) Ganges basin averaged rainfall and (b) discharge of the Ganges at Hardinge Bridge for two periods 1951–1974 (dashed) and 1975–2004 (solid). The summer discharges of the Ganges into Bangladesh before and after the construction of the Farakka Barrage are essentially the same. Winter discharge is reduced considerably.

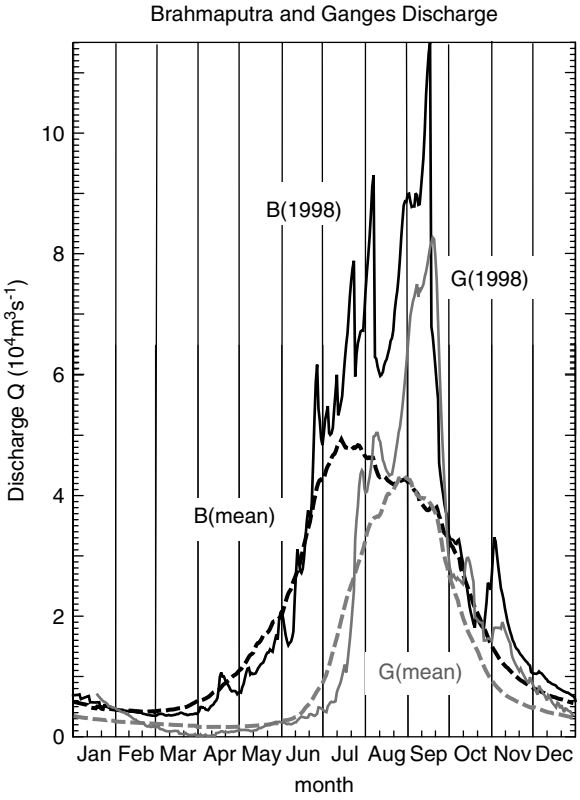

Figure 5. Detail of the Brahmaputra (black) and Ganges (grey) for 1998 measured at Bahadurabad and Hardinge Bridge. Besides exceeding the long-term averages considerably and possessing maximum amplitudes of twice the mean annual cycle (inset Figure 3(a)), there is evidence of intraseasonal variability in the discharge.

essential ingredient when designing empirical forecasting schemes for Ganges and Brahmaputra discharge.

The results of the composite analysis are confirmed by correlation analysis between pentad river discharge and pentad GPCP precipitation from 1979 to 2005. Figure 8(a) shows the correlation between wet season (June–October) Ganges River discharge and precipitation in the 3–12 pentad (15–60 days) intraseasonal for lag −4 to −1 pentads. First, the pentad river discharges are calculated from daily data corresponding to each time slot of available pentad GPCP precipitation. Then, both datasets are filtered via a moving average to remove the high and low frequency variations. The filtered pentad data in the June to October period are then used to build up a new series that is then correlated with the prior pentad precipitation (pentads −4 to −1). The results indicate that the highest positive correlation between Ganges discharge and precipitation takes place over the Ganges basin with a lag of 4 pentads (20 days) with the rainfall leading discharge. We note also that there is an in-phase relationship between rainfall over the two basins. For example, at lags −3 and −2 pentads, both basins show maximum precipitation. In addition, Figure 8(b) confirms this intraseasonal Ganges discharge–basin precipitation correlation pattern using the similar method but using the high-resolution 53-year daily precipitation $1^\circ \times 1^\circ$ dataset over India instead of the satellite-imaged rainfall dataset (Rajeevan *et al.*, 2005, 2006).

Armed with the rainfall distributions, we can now use the isochrones (Figure 2) to understand the phase similarity of the two discharge distributions on intraseasonal time-scales. The isochrones provide hydrologic support to the features observed in the composites. There is high degree of spatial coherence of the distribution of positive rainfall anomalies and their temporal occurrence (composite day) with the isochrones map. For example, for the Ganges basin, the geographic location of the rainfall anomalies at day −20 corresponds almost one-to-one with isochrones of 17 to 23 days. Similar correspondence occurs in the Brahmaputra basin.

5. Interannual variability

5.1. Seasonal discharge variability and SST:

The level of predictability of regional climate variability depends primarily on the memory of the climate system as a whole as well as on the existence and robustness of teleconnections. The memory of the climate system in seasonal to interannual time-scales is determined by the

DOI: 10.1002/qj

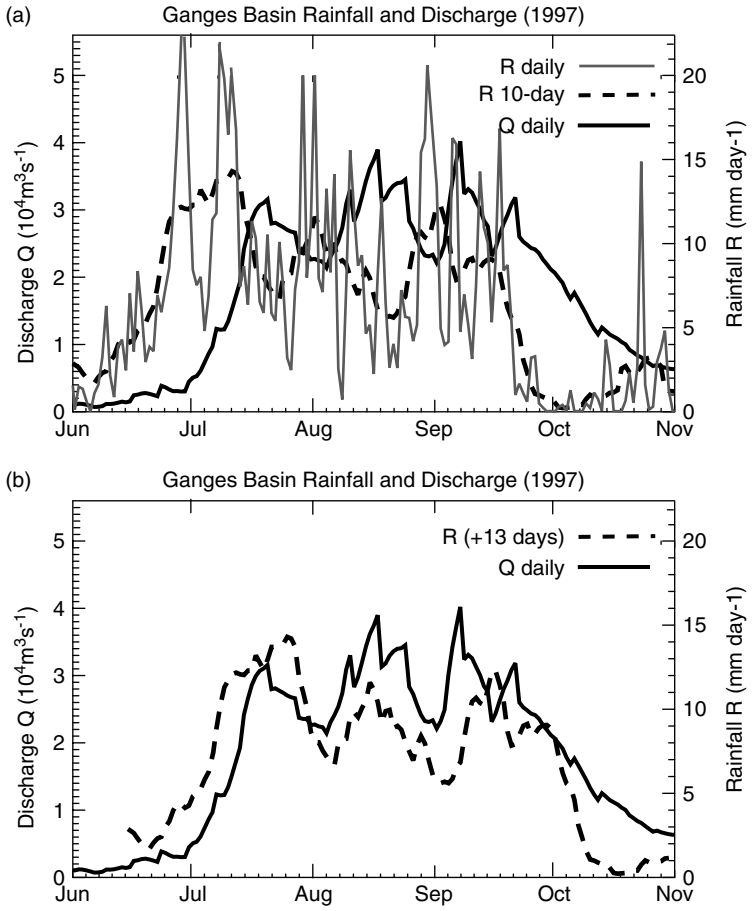

Figure 6. (a) Ganges river discharge (thick continuous line) and 10-day moving average precipitation over the basin (thick dashed line) for 1997. The thin dashed line represents the daily precipitation over the basin. (b) Rainfall distribution shifted 13 days (thick dashed line) and the Ganges discharge (thick continuous line) at Hardinge Bridge.

SST variability. For this reason, we investigate the correlations between seasonal river discharge of the Ganges and Brahmaputra rivers and global SST. From a hydrological point of view, potential relationships between SST and rainfall on seasonal time-scales are similar to those between SST and river discharge even for large basins since the hydrological time-scale of the basin (or concentration time) is shorter than the length of the season. Figure 9(a) shows correlations between the mean seasonal (July to September; JAS) Brahmaputra River discharge into Bangladesh and tropical Indo-Pacific SST on different seasonal lags using all years of available data. Shaded areas denote regions with correlation coefficients greater than 0.2. The 95% significance level ($r = 0.29$) is marked by a solid black line. The figure shows (top to bottom) simultaneous correlations, the JAS discharge and the prior April to June (AMJ) SST, and the JAS discharge with the prior January to March (JFM) SST, respectively. Overall, Figure 9(a) shows very strong and significant broad-scale correlations especially over the Indian Ocean, similar to those found by Chowdhury (2003) and Chowdhury and Ward (2004). However, from Figure 5 we note that the Brahmaputra discharge was very much stronger than average during the excessive flood year of 1998. To test the influence of this one event, the correlations were recalculated with the exclusion of 1998. Figure 9(b) indicates severely reduced correlations suggesting that 1998 contributed an overridingly strong bias to the correlations. As it turns out, the summer of 1998 was an exceptional year in terms of the magnitude of the north Indian Ocean SST anomaly (Saji *et al.*, 1999; Webster *et al.*, 1999) that reached an unprecedented 1.5 °C above normal and occurred at the time of the 1997–1998 El Niño. Whereas there is usually a warming of the Indian Ocean associated with the declining phase of an El Niño, the anomaly is generally much weaker than that which occurred during the summer of 1998.

In summary, with 1998 excluded, the SST–Brahmaputra discharge relationship is reduced to moderate regional simultaneous correlations in the Bay of Bengal. At non-zero lags, a significant correlation appears not to exist. Statistically, 1998 presents an outlier that provides little contribution to the determination of long-term predictability. We can conclude, therefore, that Brahmaputra discharge is not significantly connected to ocean SST variance over long periods. Whether or not the unique and anomalous state of the Indian Ocean during the 1998 period resulted in the excessive discharge is unclear. This question would require experimentation with numerical climate models. Irrespective of the answer, it is clear that 1998 is not representative of the

DOI: 10.1002/qj

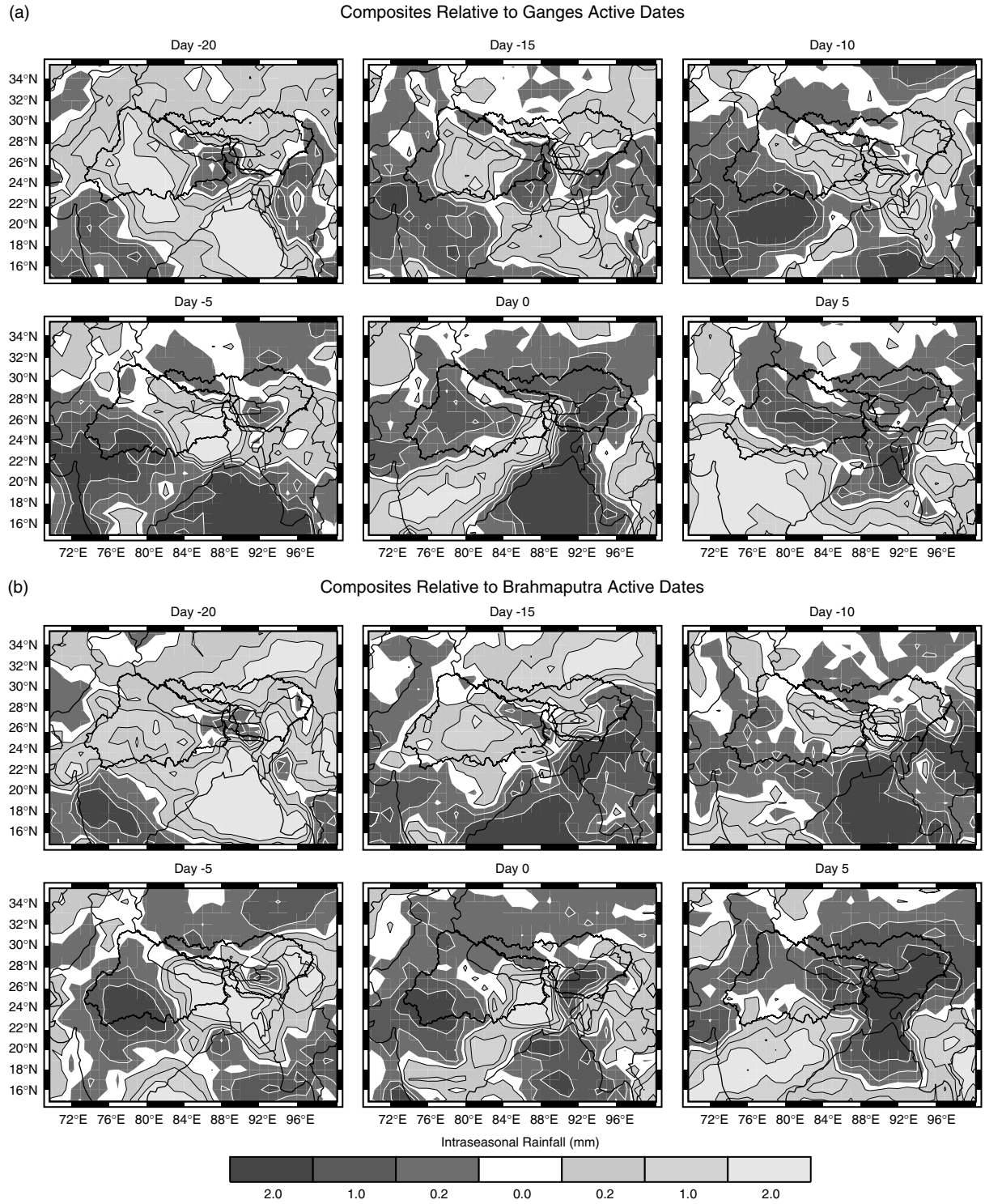

Figure 7. Evolution of the rainfall composites from day −20 to day 5 relative to (a) Ganges and (b) Brahmaputra River discharge. Shading refers to negative and positive rainfall anomalies shown at bottom of panels. Composites are defined relative to a maximum discharge at Hardinge Bridge in the 15–60 day spectral band.

long-term predictability of the Brahmaputra River discharge.

The relationship between the Ganges discharge and regional SST is very different from those found for the Brahmaputra. Maps of correlations for the same lags are displayed in Figure 9(c). In the middle and bottom panels (lag −1 and lag 0), strong negative correlations occur in the central equatorial Pacific and also eastward and to the north of the Equator. Furthermore, strong positive correlations occur in the west and southwest Pacific Ocean. The strong positive correlations over the southwest Pacific Ocean (to the east of Australia) persist throughout the correlation period commencing, in embryonic form, at −2 lags (i.e. −6 months). In addition, relatively strong

DOI: 10.1002/qj

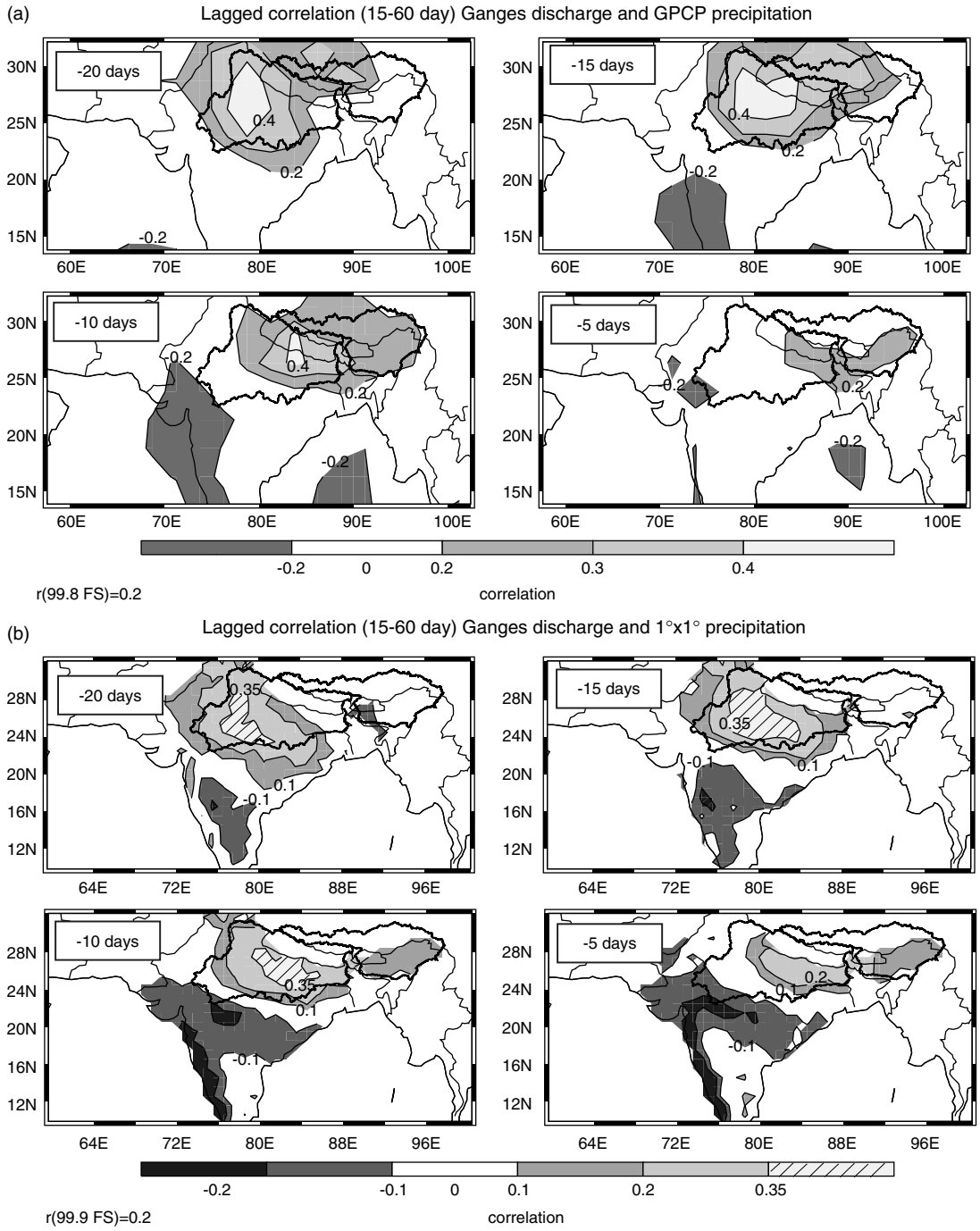

Figure 8. (a) Spatial correlation between pentad Ganges River discharge and precipitation in the intraseasonal band from pentad −4 to pentad −1 (−20 to −5 days). Both datasets are filtered in the 3–12 (15–60 day) pentad band. The correlation pattern for lags −4, −3, and −2 pentads pass the Livezey and Chen (1983) Monte Carlo field significance test at 99% level. Correlation pattern for lag −1 passes the field significance test at 95% level. (b) Same as (a) but using the daily high-resolution Indian precipitation data and daily discharge data. The correlation pattern for lags −4 and −3 pentads pass the field significance test at 99.9% level. Correlation patterns for lag −2 passes the field significance test at 99% level.

relationships exist with the equatorial northwest Pacific SST. These out-of-phase correlations between the Niño 3.4, the southwest Pacific and the northwest Pacific Ocean match the SST anomaly patterns associated with the ENSO cycle and are similar to the patterns constructed by Chowdhury and Ward (2004). Overall, the strong SST–discharge correlations one season ahead appear to suggest that useful predictability may exist for the Ganges River discharge.

It is interesting to note that there is a relative absence of correlations between Indian Ocean SST and Ganges discharge. In addition, unlike the Brahmaputra case, the exclusion of 1998 makes little difference to the correlations shown in Figure 9(c). The absence of a link with the regional SST seems strange because the Indian Ocean plays an integral part in the dynamics of the monsoon circulation through heat and moisture transfer (e.g. Webster, 1983; Webster *et al.*, 1998; Fasullo and Webster,

DOI: 10.1002/qj

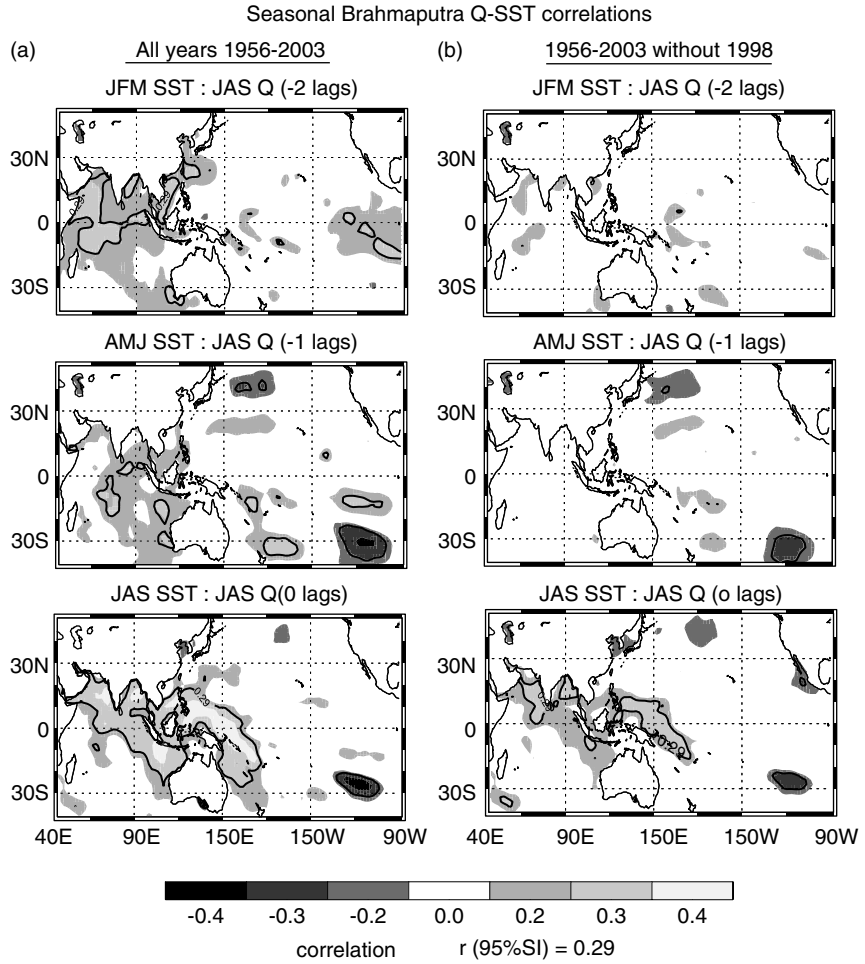

Figure 9. (a) Correlation map of JAS Brahmaputra River discharge with simultaneous SST, one-season lead (AMJ) SST, two-season lead (JFM) SST. (b) Same as (a) but with the omission of year 1998's value. (c) Same as (a) but with JAS Ganges River discharge. The significance at the 95% level is 0.29. Areas of significance are outlined by a black contour.

2002). Also, the result is not in keeping with the modest relationships between Indian Ocean SST and All-India Rainfall Index (AIRI) found by Harzallah and Sadourny (1997) and Clark *et al.* (2000, 2003). During the monsoon season, abundant rainfall keeps the soil moisture heavily saturated, thus the majority of the precipitation runs into surface runoff and finally part of river discharge. The Ganges discharge–precipitation correlation over the period 1951–2005 is very high at 0.75 between wet season mean discharge and the accumulated rainfall observed in the catchment area (76 °E–88 °E, 24°N–29°N). As the monsoon-time river discharge is highly linked to the integral of rainfall over the area of a catchment, one would expect stronger relationships with regional SST variability than that displayed in Figure 9(c). However, Harzallah and Sadourny (1997) and Clark *et al.* (2000) both sought correlations of SSTs with the All-India Rainfall Index (Parthasarathy *et al.*, 1992, 1994), the large-scale measure of total rainfall over the entire subcontinent of India. It may be that the use of such a gross rainfall index is misleading and perhaps regional correlations (e.g. Indian Ocean SST and Assam rainfall) would be consistent with the calculations made here. In fact, Webster and Hoyos (2004) noted that when district rainfall distributions were compared at the extremes of ± 1 standard deviation of the mean AIRI, there was large spatial variability of the anomalies, with states having negative anomalies in wet years and vice versa. In addition, Shukla (1995) has shown that the eastern part of the Ganges Valley is less correlated with the AIRI than the western part. In fact, towards Bangladesh the correlation actually reverses.

5.2. Monthly discharge variability and SST

The July Ganges discharge is correlated with the July (0 lag), June (-1 lags) and May (-2 lags) SSTs (Figure 10(a)) and the August discharge with August (0), July (-1) and June (-2) SSTs (Figure 10(b)). The correlation patterns are similar to those found in the seasonal calculations. The regions of high negative (positive) correlation in the central equatorial (southwest) Pacific exist for lags -2 months to lag 0. In addition, the moderate northwest Pacific correlations also persist. The highest observed correlation value of >0.6 between the May SST and Ganges discharge occurs in the southwest Pacific Ocean. The June and July Ganges basin monthly accumulated rainfall, averaged from a high-resolution daily

DOI: 10.1002/qj

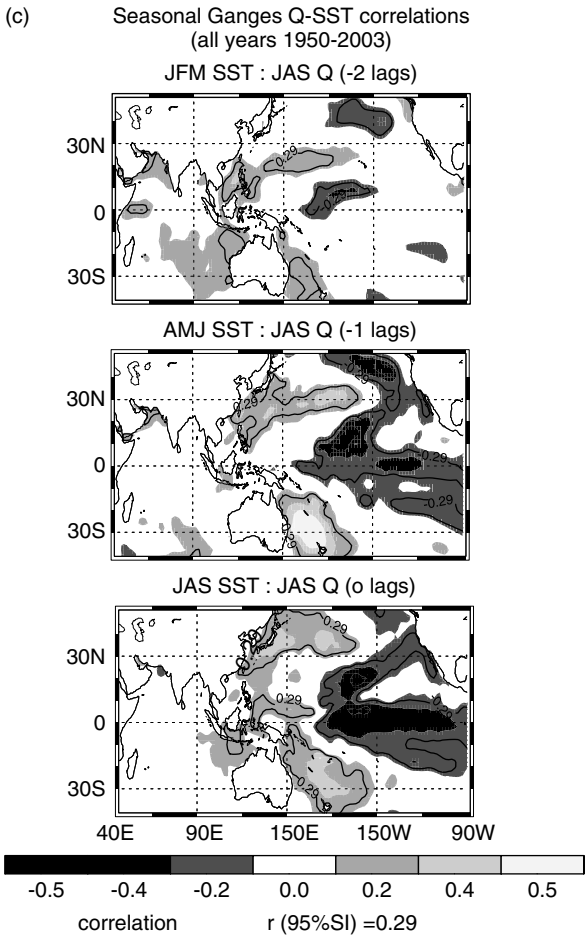

Figure 9. (*Continued*)

Indian rainfall dataset, is also found to bear a strong positive relationship with prior northwest and southwest May Pacific SSTs (Figure 10(c)). Noting that June Ganges basin rainfall correlation is stronger than July, we find out that June Ganges climatology rainfall is only half of July and August, thus the June rainfall's contribution toward discharge is relatively small. A similar analysis was conducted for the Brahmaputra discharge but periods of significance were not found. The robust leading correlation between southwest Pacific SST and summer Ganges flow may have more predictability meaning as this relationship appears to be enhanced in recent decades (Figure 10(d), the significance level is $r = 0.41$ for the 24-year period).

Figure 11 presents lead–lag correlations for the Ganges and Brahmaputra river discharge against SST in the areas of significant correlation in Figure 10. Figure 11(a) refers to associations between the discharge of the two rivers with the Niño 3.4 SST variability (120 °W–179 °W and 5°N–5 °S) and Figure 11(b) with the SST in the southwest Pacific Ocean (160 °E–180 °E, 30 °S–20 °S). The Niño 3.4 region was chosen to represent ENSO following Trenberth (1997) as being particularly sensitive to El Niño variability. The first panels (upper) of both figures show lagged correlations over a three-year period. The correlation profiles are plotted relative to the year when JAS discharges (in rectangle region) occurred. Thus Y (−1) refers to the year preceding the JAS period and Y (+1) refers to the year following it. The black dashed lines indicate the 95% significance interval. The second and third panels show the correlations between monthly discharge (lower left for July discharge and lower right for August discharge) for lags of 6 months prior to and after the discharge.

For all lags, and in all regions considered, the Brahmaputra River discharge and SST relationships do not exceed the 95% significance level. The Ganges, on the other hand, possesses stronger and more widespread relationships. For example, Figure 11(a)(upper) shows that the JAS Ganges discharge is significantly correlated with the Niño 3.4 SST from March of Y (0) through to March of Y (+1). Thus, there appears to be predictability of the JAS Ganges discharge into Bangladesh four months in advance. Figure 11(a)(upper) is similar to the lag relationships found by Yasunari (1990) between the eastern equatorial Pacific SST anomaly and Indian monsoon rainfall anomaly. Similar lag–lead relationships are found between the Ganges River discharge and the southwest Pacific Ocean SST (Figure 11(b)(upper)). The major difference between the two regions is the shape of the correlation curves. The Niño 3.4 correlations tend to increase slowly with time through year Y (0) whereas the southwest Pacific Ocean correlations change rapidly during the early spring of Y (0).

Similar correlations were found between monthly discharge and SST (lower left and lower right panels, Figs. 11(a) and (b)). The strongest relationship occurs between the southwest Pacific Ocean SST and the July Ganges discharge (Figure 11(b), lower left). At −2 lags, there is a highly significant relationship.

To demonstrate that the relationships between Pacific SST and the Ganges River discharge are not the result of individual large anomaly events or the influence of statistical outliers such as found for the Brahmaputra in 1998, scatter plots of July Ganges discharge and the SST in the two regions are shown in Figure 12. The statistics appear to be well behaved, with La Niña being associated with strong Ganges discharge and El Niño with weak discharge. This is in keeping with the relatively strong relationship between ENSO and precipitation in the upper Ganges catchment area (Shukla, 1995; Chowdhury, 2003, Chowdhury and Ward, 2004). Reversed and slightly stronger correlations exist between the Ganges discharge and the southwest Pacific Ocean SST. It should be noted, however, that not all of the variance could be explained in terms of El Niño and La Niña. There are a number of extreme discharge years that occur during non-extreme ENSO years.

Noting that there appears to be very little relationship between the ENSO phenomenon and Brahmaputra discharge, we extend the analysis to see if there are relationships with extratropical SST anomalies. Figure 13(a) shows that the June Brahmaputra River flow correlates beyond the 95% level with SST in the extratropical northwest Pacific Ocean to the east of Japan (150 °E–180 °E, 35°N–45°N) during the preceding winter and spring. Of

DOI: 10.1002/qj

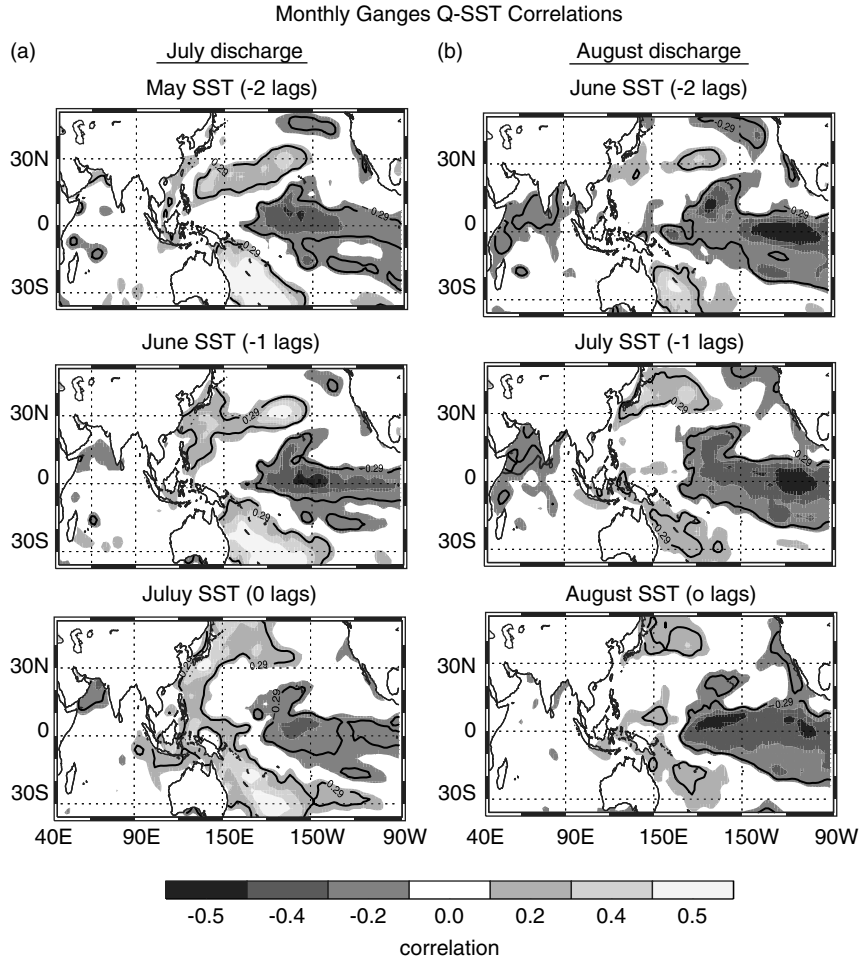

Figure 10. Correlation map of (a) July Ganges discharge with SSTs of July, June, and May over 1950–2003, (b) August Ganges discharge with SSTs of August, July, and June over 1950–2003, (c) July and June Ganges basin rainfall with May SST over 1950–2003, (d) July Ganges discharge with July SST over 1980–2003. The significance at the 95% level is 0.29. Areas of significance are outlined by a black contour.

some note is that the patterns persist for each of the lags. The maps of correlation contours and the scatter points (from May to February) are shown as a series of panels on the right-hand side in the same format as Figure 12. The correlations are not defined by outliers unlike those found earlier between the Brahmaputra discharge and the Indian Ocean SST. Correlations of the pale region inside the contour ($r = 0.4$) are locally significant at the 99% level. Figure 13(b) shows SST correlations in the Indo-Pacific region for March to June but relative to the July Brahmaputra discharge. The positive correlations in the northwest Pacific have now become negative and there are substantial areas of positive correlation spanning the Equator in the central Pacific.

We hypothesize that the changes in the sign of the Brahmaputra–SST correlation patterns are the result of two competing physical actions. Considering that a large proportion of the May and June Brahmaputra flow results from the melted snow pack over the Himalaya and the Tibetan Plateau (e.g. Shaman *et al.*, 2005), it is possible that the northwest Pacific SST is related to upstream winter storm activity that causes variations in snow pack. To some extent this contention is corroborated by SST correlations for the July Brahmaputra discharge. The positive SST correlations in the northwest Pacific (Figure 13(a)) have changed to statistically significant negative correlations. In addition, there are persistent regions of positive SST anomalies in the central Pacific spanning the Equator. These relationships match the reverse correlations between Eurasian snowfall depth and the subsequent monsoon precipitation (Blanford, 1884; Vernekar *et al.*, 1995; Bamzai and Shukla, 1999)

6. Summary

We have examined Ganges and Brahmaputra discharge at the points where they enter Bangladesh from India. These are the only two points at which staging river data are available for a long multi-decadal period. Against a background of strong and reproducible annual cycles, there is considerable variance on other time-scales. Intraseasonal monsoon precipitation variability possesses a strong signal in discharge with both basins being approximately in phase. Thus, throughout the monsoon season, active and break periods will tend to increase or decrease the total Ganges plus Brahmaputra discharge into Bangladesh. In addition, there is a high amplitude interannual variance.

DOI: 10.1002/qj

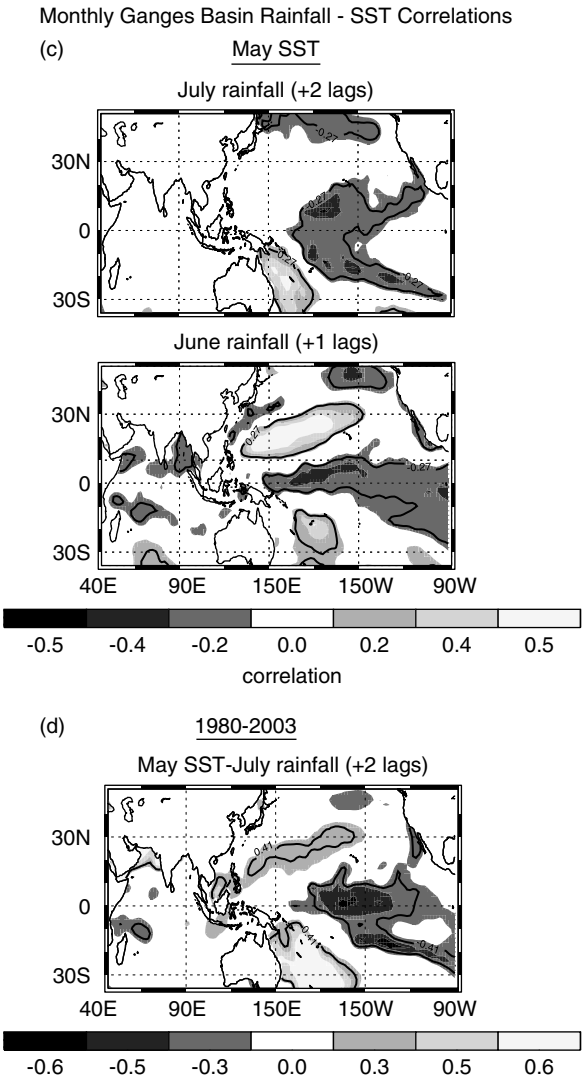

Figure 10. (*Continued*)

The association of discharge with intraseasonal variability with basin discharge suggests that there are predictable elements on these time-scales. In fact, following the band-pass rainfall over the two basins will provide a rudimentary forecast of about two to three pentads (10–15 days). To extend the forecast to longer time periods requires actual prediction of intraseasonal precipitation Webster and Hoyos (2004) employed a Bayesian scheme illustrating that there is some substantial improvements at these time-scales.

Attempts were also made to determine if the interannual variability, noted in Figure 3, was associated with large-scale climate factors. Correlation and composite analysis show that there is a significant negative linear relationship between equatorial Pacific SST and Ganges River discharge from zero to three-month lead consistent with the influence of ENSO on Indian precipitation. These results comply with those of Chowdhury and Ward (2004) and Whitaker *et al.* (2001). In addition, SSTs in the southwest Pacific Ocean show a high positive correlation with Ganges discharge, >0.6, that exists with lags for two seasons. Given the long-term relationship between northwest Indian rainfall and ENSO return to 'normality', these associations would suggest future predictability of the Ganges discharge with at least a two-month lead-time.

Contrary to the results of Chowdhury (2003) and Chowdhury and Ward (2004), no significant relationship of Brahmaputra discharge was found with tropical SSTs in either the Pacific or the Indian Oceans. The strong relationship found by earlier studies appears to come almost completely from the inclusion of year 1998 when excessive discharge occurred simultaneously with very warm Indian Ocean SSTs. With the exclusion of 1998, the strong lagged associations disappear and are replaced by minor and non-significant simultaneous correlations in the tropical Indian Ocean. It may well be that the extremely warm tropical Indian Ocean during 1998 somehow changed the circulation features of the monsoon to produce the above-average precipitation in the river basins. Irrespectively, there is no evidence that this association, if it exists, is indicative of long-term associations between the tropical Indian Ocean and Brahmaputra discharge.

In search for antecedent signals in the climate system, relationships between higher latitude SST signals and Brahmaputra discharge were sought. SST patterns to the east of Japan relate significantly to the June Brahmaputra discharge, possibly due to the SST forcing on the winter storm activities in East Asia and the increase in snow pack as suggested by Shaman *et al.* (2005). A more thorough study to seek a dynamical basis for this relationship will be carried out in the future. The reversal of the correlations perhaps reflects the anti-correlation between Eurasian spring snow cover and the following Indian summer rainfall first suggested by Blanford (1884).

Noting the particular dilemma Bangladesh faces, an attempt to provide a comprehensive forecasting system for precipitation and river discharge in the Bangladesh region is being developed under the auspices of the Climate Forecast Applications in Bangladesh (CFAB) project (Webster *et al.*, 2006; Webster *et al.*, 2009). CFAB aims to produce an overlapping three-tier set of forecasts ranging from long range (1–6 month), medium range (20–30 days) and short term (1–10 days) using post-processed European Centre for Medium-Range Weather Forecasts operational forecasts for the short term (Hopson, 2005; Hopson and Webster, 2008) and post-processed climate forecasts for the long term (Hopson, 2005). The intermediate forecast uses a physically based Bayesian scheme developed by Webster and Hoyos (2004). The concept is to provide an ability to make long-term strategic decisions with shorter-term tactical corrections. The current paper describes some of the basic science used to link river discharge with large-scale monsoon processes and climate variability.

Acknowledgements

We thank the Bangladesh Flood Forecasting and Warning Centre in Dhaka, Bangladesh for provided the daily discharge data. The NOAA Extended Reconstructed

DOI: 10.1002/qj

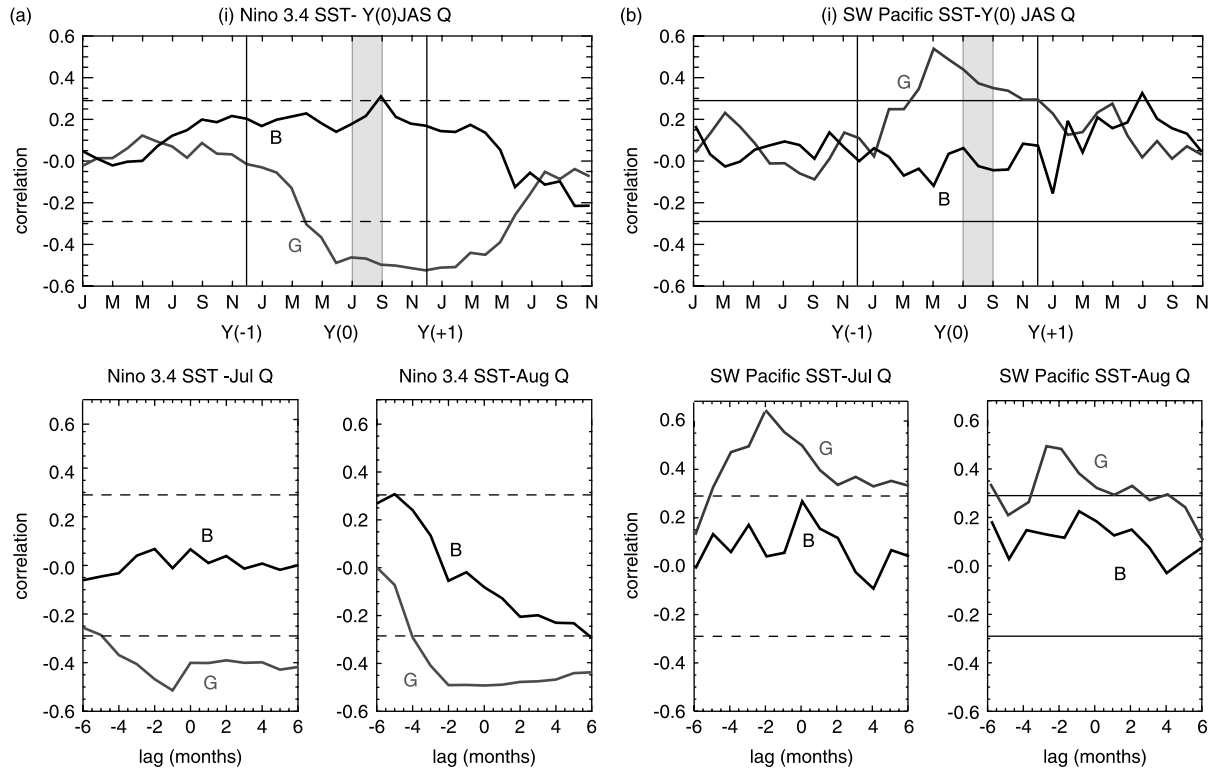

Figure 11. Systematic lagged correlations between two river discharges and (a) Niño 3.4 SST, (b) southwest Pacific SST. (Upper) seasonal (JAS) scale, (lower left) July, (lower right) August. Significance level at the 95% level is 0.29 (dashed line).

SST data are provided by the NOAA-CIRES Climate Diagnostics Center, Boulder, Colorado, USA, from their website at http://www.cdc.noaa.gov/. The GPCP satellite reanalysis data are provided by NASA Goddard Space Flight Center, USA, from their website at http://precip.gsfc.nasa.gov/. We thank the Indian Institute of Tropical Meteorology in Pune, India for the provision of the daily grid-point precipitation dataset. Funding for this work was from the Climate Dynamics section of the National Science Foundation under Grant ATM 0531771.

References

Adler RF, Huffman GJ, Chang A, Ferraro R, Xie P-P, Janowiak J, Rudolf B, Schneider U, Curtis S, Bolvin D, Gruber A, Susskind J, Arkin P, Nelkin E. 2003. The version-2 Global Precipitation Climatology Project (GPCP) monthly precipitation analysis (1979–present). *J. Hydrometeorol.* **4**: 1147–1167.

Amarasekera KN, Lee RF, Williams ER, Eltahir EAB. 1997. ENSO and the natural variability in the flow of tropical rivers. *J. Hydrol.* **200**: 24–39.

Arkin PA, Meisner BN. 1987. The relationship between large-scale convective rainfall and cold cloud over the western hemisphere during 1982–84. *Mon. Weather Rev.* **115**: 51–74.

Bamzai AS, Shukla J. 1999. Relation between Eurasian snow cover, snow depth, and the Indian summer monsoon: An observational study. *J. Climate* **12**: 3117–3132.

Blanford HF. 1884. On the connexion of the Himalaya snowfall with dry winds and seasons of drought in India. *Proc. R. Soc. London* **37**: 3–22.

Berri GJ, Ghietto MA, Garcia NO. 2002. The influence of ENSO in the flows of the Upper Paraná River of South America over the past 100 years. *J. Hydrometeorol.* **3**: 57–65.

Chow VT, Maidment DR, Mays LW. 1988. *Applied hydrology*. McGraw-Hill: New York.

Chowdhury MR. 2003. The El Niño–Southern Oscillation (ENSO) and seasonal flooding – Bangladesh. *Theor. Appl. Climatol.* **76**: 105–124.

Chowdhury MR, Ward N. 2004. Hydro-meteorological variability in the greater Ganges–Brahmaputra–Meghna basins. *Int. J. Climatol.* **24**: 1495–1508.

Clark CO, Cole JE, Webster PJ. 2000. Indian Ocean SST and Indian summer rainfall: Predictive relationships and their decadal variability. *J. Climate* **13**: 2503–2519.

Clark CO, Webster PJ, Cole JE. 2003. Interdecadal variability of the relationship between the Indian Ocean zonal mode and East African coastal rainfall anomalies. *J. Climate* **16**: 548–554.

Eldaw AK, Salas JD, Garcia LA. 2003. Long-range forecasting of the Nile River flows using climatic forcing. *J. Appl. Meteorol.* **42**: 890–904.

Fasullo J, Webster PJ. 2002. Hydrological signatures relating the Asian summer monsoon and ENSO. *J. Climate* **15**: 3082–3095.

Gershunov A, Schneider N, Barnett T. 2001. Low-frequency modulation of the ENSO–Indian monsoon rainfall relationship: Signal or noise? *J. Climate* **14**: 2486–2492.

Goswami BN, Xavier PK. 2005. ENSO control on the south Asian monsoon through the length of the rainy season. *Geophys. Res. Lett.* **32**: L18717, DOI:10.1029/2005GL023216.

Harzallah A, Sadourny R. 1997. Observed lead–lag relationships between Indian summer monsoon and some meteorological variables. *Clim. Dyn.* **13**: 635–648.

Hopson TM. 2005. 'Operational flood-forecasting for Bangladesh.' PhD thesis, Program in Atmospheric and Oceanic Sciences, University of Colorado.

Hopson TM, Webster PJ. 2009. Medium-range probabilistic river discharge forecasts for the Ganges and Brahmaputra: A template for extended hydrological flood forecasting. Submitted to *J. Hydrometeorol.*

Hoyos CD, Webster PJ. 2007. The role of intraseasonal variability in the nature of Asian monsoon precipitation. *J. Climate* **20**: 4402–4424.

Kumar KK, Rajagopalan B, Cane MA. 1999. On the weakening relationship between the Indian monsoon and ENSO. *Science* **284**: 2156–2159.

Labat D, Ronchail J, Callede J, Guyot JL, De Oliveira E, Guimarães W. 2004. Wavelet analysis of Amazon hydrological regime variability. *Geophys. Res. Lett.* **31**: L02501, DOI:10.1029/2003GL018741.

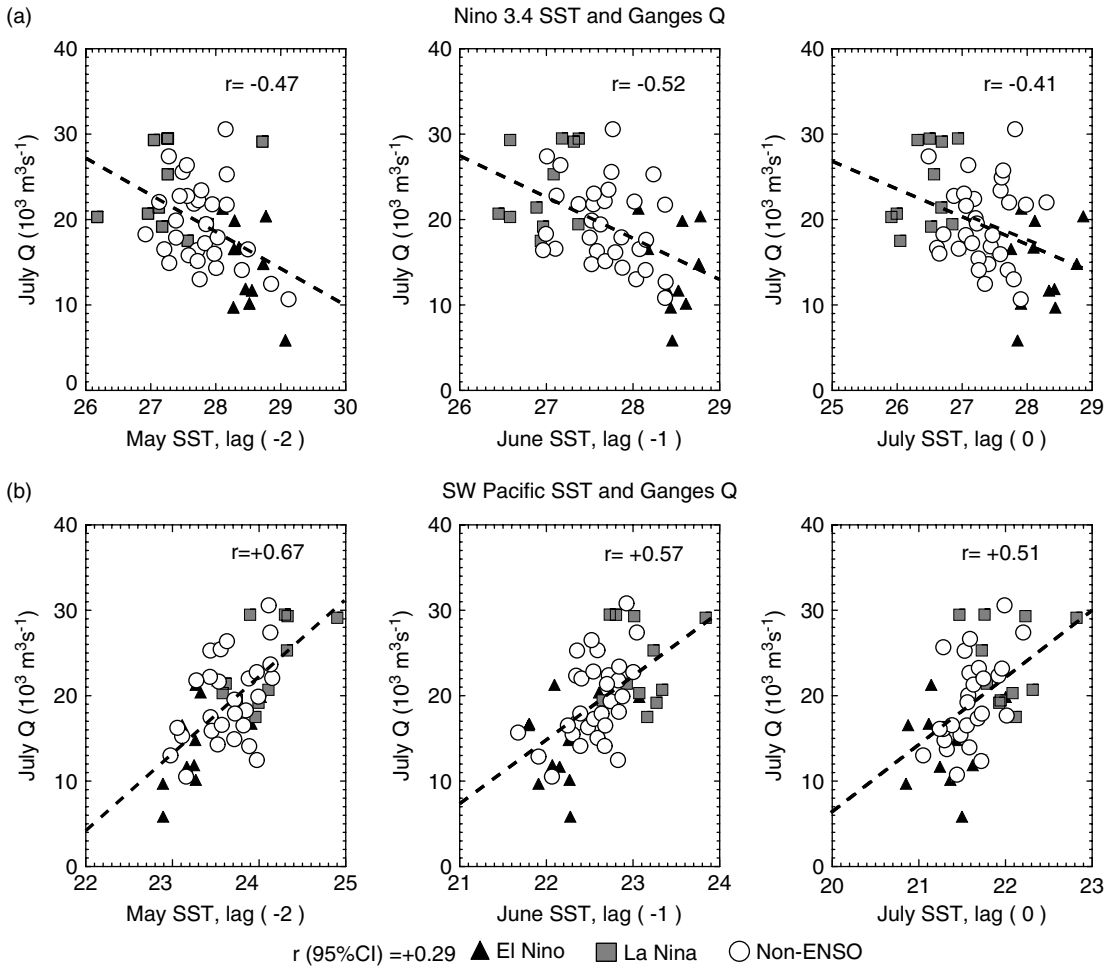

Figure 12. Regional scatter plots of (a) Niño 3.4 SST, (b) southwest Pacific SST, versus July Ganges discharge. Correlation coefficient and linear regression line are shown. Significance level at the 95% level is 0.29.

Labat D, Ronchail J, Guyot JL. 2005. Recent advances in wavelet analyses: Part 2–Amazon, Parana, Orinoco and Congo discharges time scale variability. *J. Hydrol.* **314**: 289–311.

Lawrence DM, Webster PJ. 2001. Interannual variations of the intraseasonal oscillation in the south Asian summer monsoon region. *J. Climate* **14**: 2910–2922.

Lawrence DM, Webster PJ. 2002. The boreal summer intraseasonal oscillation: Relationship between northward and eastward movement of convection. *J. Atmos. Sci.* **59**: 1593–1606.

Livezey RE, Chen WY. 1983. Statistical field significance and its determination by Monte Carlo techniques. *Mon. Weather Rev.* **111**: 46–59.

Madden RA, Julian PR. 1994. Observations of the 40–50-day tropical oscillation: A review. *Mon. Weather Rev.* **122**: 814–837.

Mirza MMQ, Warrick RA, Ericksen NJ. 2003. The implications of climate change on floods of the Ganges, Brahmaputra and Meghna rivers in Bangladesh. *Clim. Change* **57**: 287–318.

Normand C. 1953. Monsoon seasonal forecasting. *Q. J. R. Meteorol. Soc.* **79**: 463–473.

Parthasarathy B, Kumar KR, Kothawale DR. 1992. Indian summer monsoon indices: 1871–1990. *Meteorol. Mag.* **121**: 174–186.

Parthasarathy B, Munot AA, Kothawale DR. 1994. All-India monthly and seasonal rainfall series: 1871–1993. *Theor. Appl. Climatol.* **49**: 217–224.

Ramirez JM, Vélez JI. 2002. Estrategias para la estimacion automatica de direcciones de drenaje a partir de modelos digitales de terreno (Strategies of automated drainage directions extraction from digital elevation models). *Avances en Recursos Hidráulicos* **9**: 45–63.

Rajeevan M, Bhate J, Kale JD, Lal B. 2005. 'Development of a high resolution daily gridded rainfall data for the Indian region.' Met. Monograph Climatology No. 22/2005, pp. 26. India Meteorological Department, Pune.

Rajeevan M, Bhate J, Kale JD, Lal B. 2006. High resolution daily gridded rainfall data for the Indian region: Analysis of break and active monsoon spells. *Current Science (Bangalore)* **91**: 296–306.

Saji NH, Goswami BN, Vinayachandran PN, Yamagata T. 1999. A dipole mode in the tropical Indian Ocean. *Nature* **401**: 360–363.

Shaman J, Cane M, Kaplan A. 2005. The relationship between Tibetan snow depth, ENSO, river discharge and the monsoons of Bangladesh. *Int. J. Remote Sensing* **26**: 3735–3748.

Shukla J. 1995. 'Predictability of the tropical atmosphere, the tropical oceans and TOGA.' Pp. 725–730 in Proc. International Conference on the Tropical Ocean–Global Atmopshere (TOGA) Programme, Vol. 2, WCRP-91, WMO/TD 717. World Climate Research Programme, Geneva, Switzerland.

Shukla J, Paolino DA. 1983. The southern oscillation and long-range forecasting of the summer monsoon rainfall over India. *Mon. Weather Rev.* **111**: 1830–1837.

Sikka DR, Gadgil S. 1980. On the maximum cloud zone and the ITCZ over Indian longitudes during the southwest monsoon. *Mon. Weather Rev.* **108**: 1840–1853.

Smith TM, Reynolds RW. 2003. Extended reconstruction of global sea surface temperatures based on COADS data (1854–1997). *J. Climate* **16**: 1495–1510.

Stephenson DB, Kumar KR, Doblas-Reyes FJ, Royer J-F, Chauvin F, Pezzulli S. 1999. Extreme daily rainfall events and their impact on ensemble forecasts of the Indian monsoon. *Mon. Weather Rev.* **127**: 1954–1966.

Subbiah A (Ed). 2004. 'Initial report on the Indian monsoon drought of 2002.' Asian Disaster Preparedness Centre, Technical Report, Bangkok, Thailand, 29 pp.

Tawfik M. 2003. Linearity versus non-linearity in forecasting Nile River flows. *Adv. Eng. Software* **34**: 515–524.

DOI: 10.1002/qj

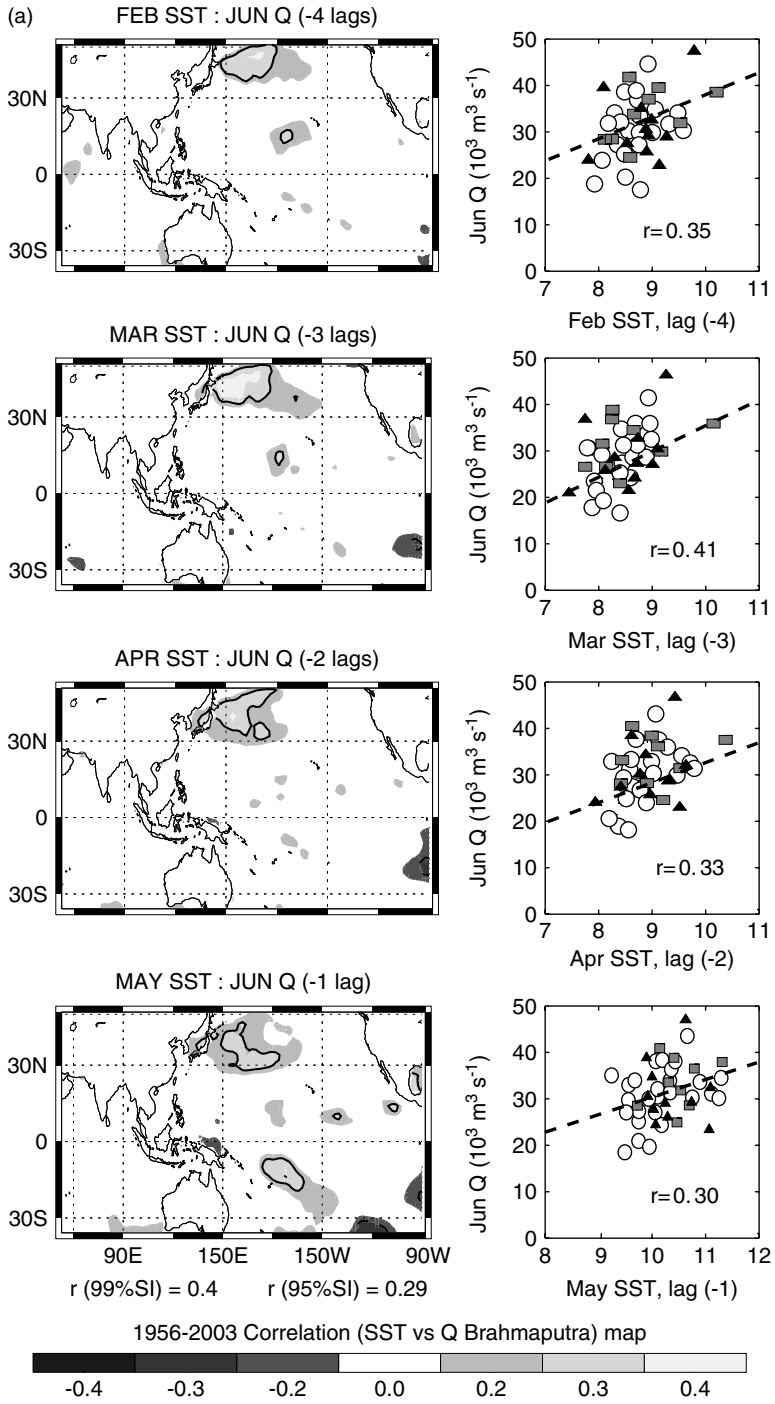

Figure 13. (a) Correlation between June Brahmaputra discharge and northwest Pacific SST. Left panel shows the correlation map between discharge and previous monthly SSTs (February to May); right panel shows the scatter plots between the two variables, respective to the left. (b) Same as (a) but between the July Brahmaputra discharge and previous monthly (March to June) SSTs, also with the exclusion of 1998's value. Significance level at the 95% level is 0.29 and is shown as a solid contour.

Torrence C, Webster PJ. 1998. The annual cycle of persistence in the El Niño–Southern Oscillation. *Q. J. R. Meteorol. Soc.* **124**: 1985–2004.

Torrence C, Webster PJ. 1999. Interdecadal changes in the ENSO–monsoon system. *J. Climate.* **12**: 2679–2690.

Trenberth KE. 1997. The definition of El Niño. *Bull. Am. Meteorol. Soc.* **78**: 2771–2777.

van Oldenborgh GJ, Burgers G. 2005. Searching for decadal variations in ENSO precipitation teleconnections. *Geophys. Res. Lett.* **32**: L15701, DOI:10.1029/2005GL023110.

Vernekar AD, Zhou J, Shukla J. 1995. The effect of Eurasian snow cover on the Indian monsoon. *J. Climate* **8**: 248–266.

Wang G, Eltahir EAB. 1999. Use of ENSO information in medium- and long-range forecasting of the Nile floods. *J. Climate* **12**: 1726–1737.

Webster PJ. 1983. Mechanisms of monsoon low-frequency variability: Surface hydrological effects. *J. Atmos. Sci.* **40**: 2110–2124.

Webster PJ, Hoyos C. 2004. Prediction of monsoon rainfall and river discharge on 15–30-day time scales. *Bull. Am. Meteorol. Soc.* **85**: 1745–1765.

Webster PJ, Yang S. 1992. Monsoon and ENSO: Selectively interactive systems. *Q. J. R. Meteorol. Soc.* **118**: 877–926.

Webster PJ, Magaña VO, Palmer TN, Shukla J, Tomas RA, Yanai M, Yasunari T. 1998. Monsoons: Processes, predictability, and the prospects for prediction. *J. Geophys. Res.* **103**(C7): 14451–14510.

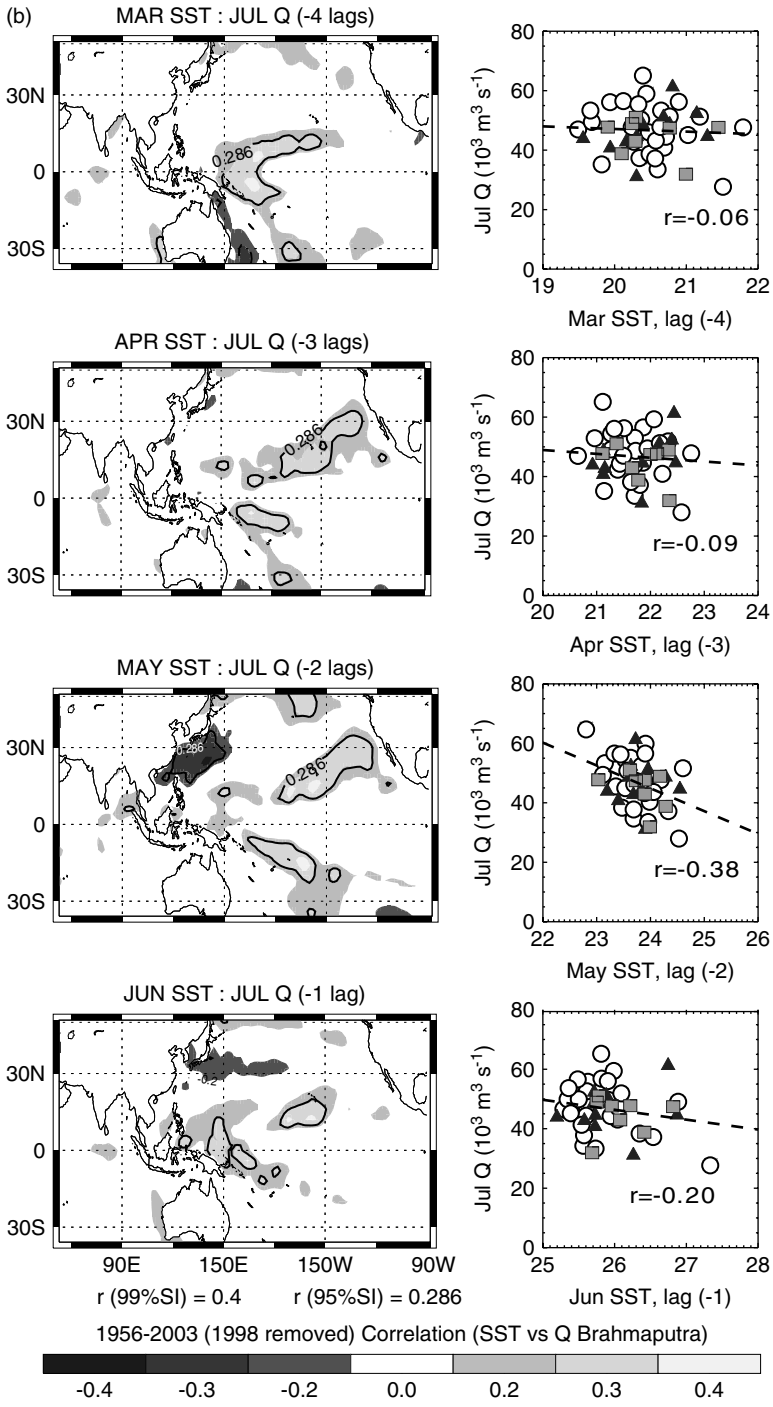

Figure 13. (*Continued*)

Webster PJ, Moore AM, Loschnigg JP, Leben RR. 1999. Coupled ocean–atmosphere dynamics in the Indian Ocean during 1997–98. *Nature* **401**: 356–360.

Webster PJ, Hopson T, Hoyos C, Subbiah A, Chang H-R, Grossman R. 2006. A three-tier overlapping prediction scheme: Tools for strategic and tactical decisions in the developing world. Chapter 26 in *Predictability of Weather and Climate*, Palmer TN, Hagedorn R (Eds). Cambridge University Press: New York.

Webster PJ, Hopson TM, Hoyos CD, Jian J, Chang H-R, Agudelo PA. 2009. Extended range probabilistic forecasting of the 2007 Bangladesh floods. Submitted to *Nature* Geoscience.

Whitaker DW, Wasimi SA, Islam S. 2001. The El Niño–Southern Oscillation and long-range forecasting of flows in the Ganges. *Int. J. Climatol.* **21**: 77–87.

Yasunari T. 1990. Impact of Indian monsoon on the coupled atmosphere/ocean system in the tropical Pacific. *Meteorol. Atmos. Phys.* **44**: 29–41.

DOI: 10.1002/qj